

**Synthesis of bulk chromium hydrides under pressure of up to 120 GPa**Adrien Marizy, Grégory Geneste, and Paul Loubeyre\*  
CEA, DAM, DIF, F-91297 Arpajon, FranceBastien Guigue  
CEA, DAM, DIF, F-91297 Arpajon, France  
and LPEM, ESPCI Paris, PSL Research University, CNRS, Sorbonne Université, 75005 Paris, FranceGaston Garbarino  
ESRF, The European Synchrotron, 71 Avenue des Martyrs, 38000 Grenoble, France

(Received 6 March 2018; revised manuscript received 26 April 2018; published 18 May 2018)

Stable compounds in the Cr-H system have been synthesized through a direct reaction of chromium and hydrogen in a laser-heated diamond-anvil cell and investigated using synchrotron x-ray diffraction up to 120 GPa. The sequence of hydrides CrH, Cr<sub>2</sub>H<sub>3</sub>, and CrH<sub>2</sub> has been observed by increasing pressure. The known  $\epsilon$ -hcp-CrH hydride is formed above 3 GPa. A Cr<sub>2</sub>H<sub>3</sub> hydride with a *C2/m* structure appears spontaneously above 19 GPa, as a result of the filling of the tetrahedral sites of  $\epsilon$ -CrH. YAG laser heating helps dissolve more hydrogen inside the hcp chromium structure to synthesize a CrH<sub>2</sub> compound with a *Pnma* structure from 30 GPa on. The volume expansion per hydrogen atom in octahedral and tetrahedral sites is measured up to the 100-GPa pressure range. The formation pressures and structures of these chromium interstitial hydrides are in very good agreement with DFT calculations. However, despite multiple heating attempts up to 100 GPa, no evidence of the stability of the predicted CrH<sub>3</sub> compound could be found.

DOI: [10.1103/PhysRevB.97.184103](https://doi.org/10.1103/PhysRevB.97.184103)**I. INTRODUCTION**

Over the past decade, many calculations have revealed that the hydrogen content in metals should dramatically increase at high pressure. Under pressures of a few tens of GPa, many elements have been predicted to form hydrides with unconventionally high hydrogen stoichiometries [1–3]. Furthermore, these polyhydrides hold great promise as a class of potential high-temperature superconductors [3,4] especially with the recent observation of a superconductivity in compressed hydrogen sulfide at a  $T_c$  of 203 K at 150 GPa which could be explained by the formation of H<sub>3</sub>S [5]. Up to now, however, few experiments have been performed to test the large corpus of predictions available in the literature. It is important to collect more experimental data to assess the reliability of these *ab initio* predictions. In this context, the investigation of transition-metal polyhydrides seems promising especially, since a sequence of iron hydrides, FeH, FeH<sub>2</sub>, FeH<sub>3</sub>, and FeH<sub>5</sub>, has been recently discovered by increasing pressure in the Fe-H system [6,7].

Transition-metal hydrides have been studied for decades and exhibit a close-packed metal host lattice with hydrogen in interstitial sites. These hydrides usually have a hydrogen:metal (H:M) ratio close to 1, with few exceptions of higher ratio [8]. Until recently, dihydrides (H:M ratio = 2) were known only for five transition metals from groups IV and V (Ti, Zr, Hf, V, and Nb) and were synthesized at ambient pressure. By

compressing metals embedded in hydrogen using a diamond-anvil cell, other dihydrides were discovered: TaH<sub>2</sub> at 5 GPa [9]; RhH<sub>2</sub> at 8 GPa [10]; FeH<sub>2</sub> above 67 GPa [7]. The discovery of trihydrides (M:H ratio = 3) really demonstrates that pressure can change the nature of transition-metal hydrides from interstitial to reorganized, as observed for three metals: IrH<sub>3</sub> above 55 GPa [11], FeH<sub>3</sub> above 85 GPa [7] and NbH<sub>3</sub> above 56 GPa [4]. According to calculations, group VI seems very promising to observe a rich variety of polyhydrides under pressure, up to stoichiometries as high as 8 [3,12,13]. But, surprisingly, molybdenum and tungsten did not even form dihydrides at pressures well above their predicted stability pressure [12,14,15]. Here, the formation of polyhydrides of another group-VI transition *d* metal, chromium, is investigated.

Indeed, many hydrogen atoms can be bound to a chromium atom, as molecular complexes up to (H<sub>2</sub>)<sub>2</sub>CrH<sub>2</sub> have already been detected through the condensation of chromium vapors in solid gas matrices at a few K [16,17] and a DFT study even predicts the existence of CrH<sub>12</sub> molecules [18]. In the solid state, as early as 1926, chromium has been reported to form hydrides with up to three hydrogen atoms for one chromium atom [19]. This claim has not been confirmed in later experiments but solid bulk layers of CrH (and possibly also of CrH<sub>1.7</sub>) were synthesized electrochemically [20–23]. Their structure is either *hcp* or *fcc*, depending on the condition of cathodic electrodeposition [21,24,25]. In 1998, the compression curves of these two types of electrodeposited chromium hydrides were measured up to 40 GPa [26]. The synthesis of the hcp  $\epsilon$ -CrH (perfect anti-NiAs-type) hydride from bulk chromium and hydrogen and its study up to 1.6 GPa was

\*paul.loubeyre@cea.fr

performed by Baranowski in 1972 [27,28] and subsequently by Ponyatovsky in 1976 [29]. Then, in 2002, the stability of *hcp* CrH was studied versus temperature ( $T > 500$  K) and pressure up to 6 GPa [30]. A phase transition toward the *fcc*  $\gamma$  phase was found as the temperature was increased but these results are questioned by a thermodynamic study [31] and a recent experimental investigation of the Mo-H system which did not confirm the formation of the high-pressure high-temperature *fcc* MoH hydride [32].  $\epsilon$ -CrH is an interstitial hydride with H atoms occupying the octahedral sites of the *hcp* chromium lattice [33]. According to a recent theoretical paper by Yu *et al.* a variety of  $\text{CrH}_x$  hydrides should form under pressure, giving rise to interstitial hydrides but also to compounds in which hydrogen acts as a bridging atom between chromium atoms [13]. More than five interesting stable stoichiometries have been predicted, the highest stoichiometry calculated being  $\text{CrH}_8$  above 130 GPa. Moreover, CrH and  $\text{CrH}_3$  have been calculated to be superconductors with a transition temperature around 10 K at ambient pressure and 40 K at 80 GPa, respectively [13].

We report below the formation of two bulk chromium hydrides,  $\text{Cr}_2\text{H}_3$  and  $\text{CrH}_2$ , by direct reaction of Cr and H in a diamond-anvil cell. These are two interstitial hydrides. However, the formation of the  $\text{CrH}_3$  compound was not observed in its predicted stability pressure range. *Ab initio* calculations are also presented to extend the comparison between experiment and calculations.

## II. METHODS

Three pressure runs were performed on chromium-hydrogen samples loaded in a diamond-anvil cell. Different diamond-anvil cuts were used to cover different pressure ranges: culets of 400  $\mu\text{m}$  (run 1), 300  $\mu\text{m}$  (run 2), and 150  $\mu\text{m}$  (run 3). The rhenium gasket was covered by 100 nm of gold to limit hydrogen diffusion. Hydrogen was loaded in the diamond anvil cell (DAC) under 1400 bars. As shown by the photograph in Fig. 1, the chromium flake was surrounded by an excess of hydrogen, even up to the maximum pressure investigated, to be able to synthesize the polyhydride with the highest fraction of hydrogen stable at a given pressure. A gold marble was loaded next to the sample and the pressure was measured with the equation of state of gold, as defined in [34]. The diffraction patterns were collected using a MARCCD detector at the ID27 beamline at the ESRF with a wavelength of 0.3738  $\text{\AA}$ . For each run, the sample was heated by a YAG laser at different pressures, as indicated in Fig. 1, to accelerate the kinetics of hydrogen diffusion in the chromium sample. Different colors are used for three types of laser heating session: a low-temperature one ( $T < 800$  K), a midtemperature one ( $800 \text{ K} < T < 1200$  K) and a high-temperature one ( $1200 \text{ K} < T < 1500$  K). The temperatures are just rough estimates, obtained from the thermionic emission observed. It is important to note that the laser heating had to be long enough to complete the transformation of the sample but not too long to obtain a powder that is not too textured, to be able to perform Rietveld refinements of the synthesized structure later on. In run 2, the stability of the chromium hydrides has also been investigated upon decreasing pressure. The DIOPAS software [35] and the FULLPROF package [36] were used to

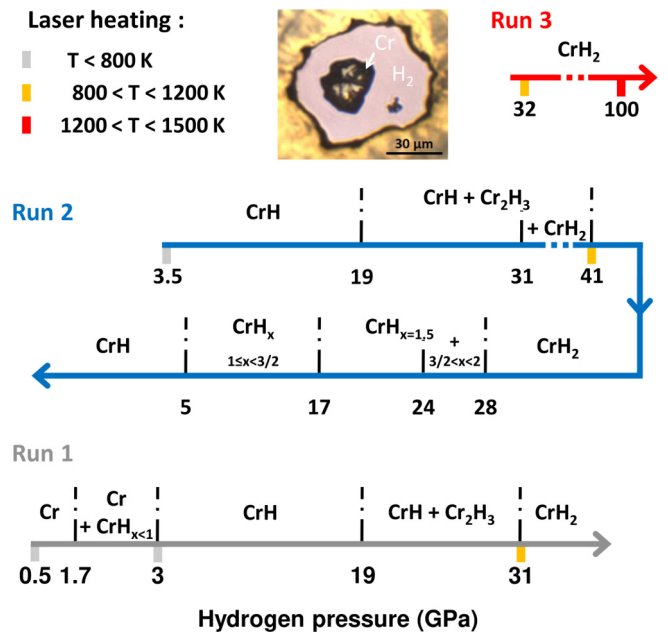


FIG. 1. Schematic representation of the different experimental runs and of the pressure stability ranges of CrH,  $\text{Cr}_2\text{H}_3$ ,  $\text{CrH}_2$  embedded in hydrogen. Upon pressure decrease in run 2, intermediate hydrogen concentrations were observed probably due to a slow kinetics of hydrogen diffusion out of the hydrides.

analyze the recorded x-ray-diffraction data. The uncertainty in pressure is  $\pm 3\%$  and in volume  $\pm 0.09 \text{ \AA}^3/\text{Cr}$ .

Calculations were also performed to complement Yu *et al.*'s data [13] especially for compression curves and formation enthalpies of the various synthesized chromium hydrides. Ground-state DFT calculations have been performed with the ABINIT code [37] using optimized norm-conserving Vanderbilt pseudopotentials (ONCVSP) [38]. The generalized gradient approximation in the Perdew-Burke-Ernzerhof form (GGA-PBE) [39] was employed. The lattice parameters and the atomic positions of Cr, CrH,  $\text{Cr}_2\text{H}_3$ ,  $\text{CrH}_2$ ,  $\text{CrH}_3$ ,  $\text{CrH}_4$ , and  $\text{CrH}_8$  were optimized as a function of hydrostatic pressure. A  $k$ -point grid of  $40 \times 40 \times 40$  for Cr,  $40 \times 40 \times 25$  for CrH,  $15 \times 40 \times 25$  for  $\text{Cr}_2\text{H}_3$ ,  $25 \times 40 \times 25$  for  $\text{CrH}_2$ ,  $30 \times 30 \times 40$  for  $\text{CrH}_3$ ,  $30 \times 30 \times 15$  for  $\text{CrH}_4$ , and  $25 \times 25 \times 30$  for  $\text{CrH}_8$  was used along with a plane-wave cutoff of 50 Ha (convergence tests with a plane-wave cutoff of 60 Ha were performed in selected cases, providing identical formation enthalpies with differences much smaller than 1 meV/atom). No magnetism was taken into account, as Yu *et al.* have demonstrated that it had no influence [13].

## III. CHROMIUM HYDRIDES

The formation of three chromium hydrides, CrH,  $\text{Cr}_2\text{H}_3$ , and  $\text{CrH}_2$ , has been reproducibly observed during the three runs through compression and decompression paths, as summarized in Fig. 1. For each new hydride, x-ray-diffraction patterns revealed powders of sufficient quality to be able to perform a Rietveld refinement of the structural positions of the Cr atoms. The hydrogen stoichiometry was estimated from the volumetric expansion caused by the hydrogen insertion

inside the chromium lattice and the structural positions of the hydrogen atoms were assumed to be those given by *ab initio* calculations from Yu *et al.* [13].

### A. CrH

Below 1 GPa, chromium embedded in hydrogen remains in the *bcc* phase, even after a few days. No volume difference, within the experimental uncertainty, was noticed with *bcc* chromium embedded in a helium pressure-transmitting medium, which is in agreement with the calculated solubility of hydrogen in chromium, i.e.,  $x \sim 2.10^{-5}$  at 500 K and 1 GPa [40]. By laser heating the chromium sample at 0.5 GPa and at a temperature inferior to 800 K, a single crystal of *bcc* chromium formed. Indeed,  $\epsilon$ -CrH is not stable at a temperature superior to 500 K at this pressure according to the already published data on the Cr-H system [30]. Above 1.7 GPa, small *hcp* peaks appear along with the main peaks of *bcc* chromium in the x-ray pattern, indicating the formation of a hexagonal close-packed  $\text{CrH}_x$  hydride. Laser-heating at 3 GPa leads to a complete transformation of the sample into  $\epsilon$ -CrH with a volume slightly higher than that of the *hcp*  $\text{CrH}_x$  phase formed by the sole

pressure increase. The hydrogen content before heating is estimated to be  $x = 0.96$  which corresponds to what is often found by electrochemical synthesis. A Rietveld refinement of the integrated x-ray-diffraction pattern was successfully performed in the  $P6_3/mmc$  space group with Cr atoms in position  $2c$ , as can be seen in Fig. 2(b). As shown below, the volume expansion of the Cr lattice due to hydrogen dissolution corresponds well to the filling of the octahedral site of the *hcp* lattice. Upon pressure decrease, CrH was recovered metastable at ambient pressure, as expected.

### B. $\text{Cr}_2\text{H}_3$

Under further pressure increase, new diffraction peaks appeared above 19 GPa. The diffraction pattern can be interpreted as a mixture of CrH and the predicted  $\text{Cr}_2\text{H}_3$ . A pure  $\text{Cr}_2\text{H}_3$  phase was obtained during pressure decrease from 24 GPa and a Rietveld refinement of the corresponding integrated x-ray-diffraction pattern was performed in the  $C2/m$  space group. Chromium atoms were found to be in position  $4i$  [(0.883, 0, 0.266) and (0.379, 0, 0.795)], as shown in Fig. 2(c). This structure matches Yu *et al.*'s predictions [13] for the

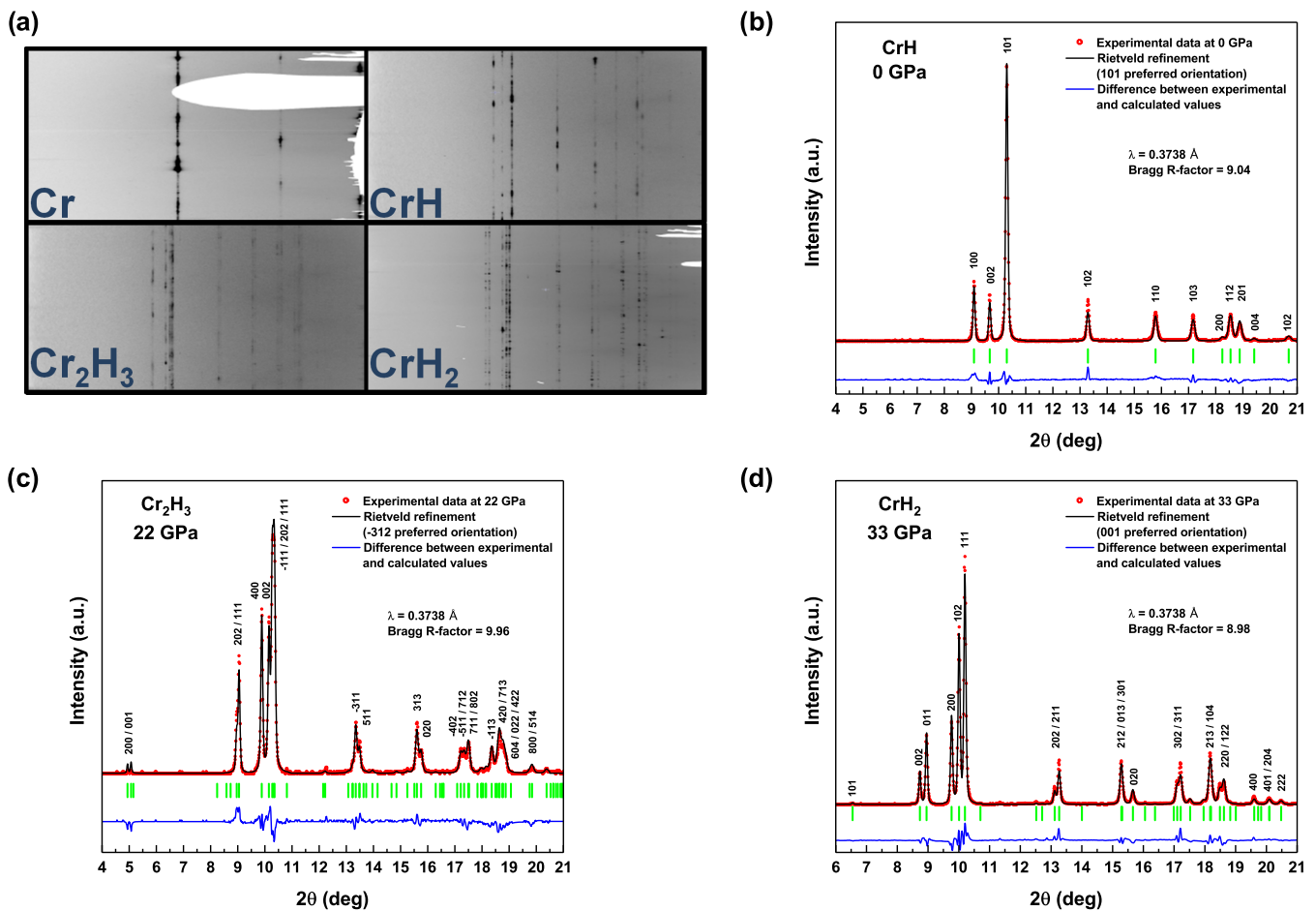


FIG. 2. (a) Unrolled recorded XRD image for each hydrogen stoichiometry. (b) Rietveld refinement of CrH after complete pressure release [ $P6_3/mmc$ ,  $a = b = 2.722 \text{ \AA}$ ,  $c = 4.433 \text{ \AA}$  with Cr atoms in position  $2c$ , (101) as preferred orientation]. (c) Rietveld refinement of  $\text{Cr}_2\text{H}_3$  at 22 GPa on pressure release [ $C2/m$ ,  $a = 9.828 \text{ \AA}$ ,  $b = 2.727 \text{ \AA}$ ,  $c = 4.787 \text{ \AA}$ ,  $\beta = 61.99^\circ$  with Cr atoms in position  $4i$  (0.883,0,0.266) and (0.379,0,0.795), (−312) as preferred orientation]. (d) Rietveld refinement of  $\text{CrH}_2$  at 33 GPa [ $Pnma$ ,  $a = 4.391 \text{ \AA}$ ,  $b = 2.744 \text{ \AA}$ ,  $c = 4.909 \text{ \AA}$  with Cr atoms in position  $4c$  (0.259, 0.75, 0.590), (110) as preferred orientation].

H:Cr = 1.5:1 hydride. As discussed below, the volume expansion due to the dissolution of more hydrogen in the *hcp* chromium lattice corresponds, this time, to the partial filling of the tetrahedral sites. Upon decreasing pressure, the emergence of new nonindexed diffraction peaks in the diffraction pattern below 17 GPa indicates a desorption process of Cr<sub>2</sub>H<sub>3</sub> into CrH (for which the corresponding diffraction peaks appear from 11 GPa in the mixture). This desorption process was completed at 5 GPa, with only the diffraction peaks of  $\epsilon$ -CrH present in the pattern. Hence, the stability pressure of Cr<sub>2</sub>H<sub>3</sub> ranges from 17 to 24 GPa with slight hysteresis at the transition between CrH and Cr<sub>2</sub>H<sub>3</sub> (17–19 GPa).

### C. CrH<sub>2</sub>

If no laser heating is applied to the sample, from 31 GPa on, the diffraction pattern was interpreted as a mixture between three phases: CrH, Cr<sub>2</sub>H<sub>3</sub>, and CrH<sub>2</sub>. After moderate laser heating, a complete transformation of the sample into pristine CrH<sub>2</sub> was observed. A Rietveld refinement of the integrated x-ray-diffraction pattern, as shown in Fig. 2(d) was performed in the *Pnma* space group with chromium atoms in position 4c (0.259, 0.75, 0.590) which fits in well with Yu *et al.*'s predictions [13]. A pressure increase up to 120 GPa did not show any sign of the spontaneous apparition of a new phase. The CrH<sub>2</sub> phase remains the most stable one even under high-temperature and persistent laser-heating of the sample at 100 GPa. We can thus state that CrH<sub>2</sub> is the chromium hydride of highest stoichiometry that can be synthesized in the Cr-H system up to 100 GPa. Upon pressure decrease, CrH<sub>2</sub> started to release its hydrogen below 28 GPa and went back to Cr<sub>2</sub>H<sub>3</sub> at 24 GPa. Again, the hysteresis of the transition between CrH<sub>2</sub> and Cr<sub>2</sub>H<sub>3</sub> is small, 28–31 GPa.

## IV. DISCUSSION

### A. Compression curve

The compression data,  $V(P)$ , for CrH, Cr<sub>2</sub>H<sub>3</sub>, and CrH<sub>2</sub> in a hydrogen pressure transmitting medium is plotted in Fig. 3. The compression data of chromium in a helium pressure transmitting medium is also plotted to visualize the volume expansion per formula unit associated with the hydrogen content increase. The compression curves at  $T = 0$  K for these various compounds have been calculated and are plotted for comparison. The Vinet equation of state function is used to fit all these data. Robust values of the initial volume  $V_0$ , initial bulk modulus  $B_0$ , and its pressure derivative  $B'_0$  are usually obtained and are reported in Table I. Previous experimental  $V(P)$  data from Tkacz *et al.* [26] shows less compressible Cr and CrH compounds with increasing deviation from our data as pressure increases. However, that is probably due to the presence (our data) or absence (Tkacz *et al.*'s data) of a quasihydrostatic pressure medium. As seen in Table I, adding H atoms to Cr significantly lowers the bulk modulus. CrH<sub>2</sub> is significantly more compressible than CrH that is itself more compressible than Cr. This is in agreement with previous measurements in the Fe-H system, FeH<sub>2</sub> and FeH exhibiting significantly lower bulk moduli than Fe, respectively 127, 131, and 163 GPa [7]. But this differs from the traditional low-pressure view on interstitial hydrides: essentially, in interstitial sites,

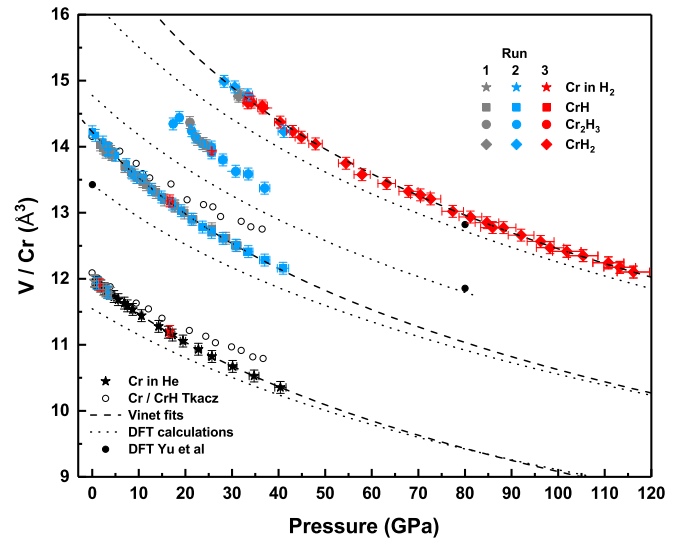


FIG. 3. Atomic volume as a function of pressure. The uncertainty in pressure is  $\pm 3\%$  and in volume  $\pm 0.09 \text{ \AA}^3/\text{Cr}$ .

hydrogen is assumed to appear mostly incompressible and so the mechanical behavior of the hydride should be almost identical to the one of the parent metal. Yet, that view seems to apply for two recent high-pressure studies, one on TaH<sub>2</sub> [15] and the other on NbH<sub>2</sub> [4]. However, in our study, as shown below, the lattice expansion due to hydrogen dissolution is a clear decreasing function of pressure, so that hydrogen is indeed compressible in interstitial sites.

As seen in Fig. 3, the calculated compression curves, obtained by the *ab initio* structural optimization at different pressures, systematically underestimate the volume of all the chromium hydrides but also of pure chromium with an error between 4 and 6% at ambient pressure. Yet, this underestimation decreases with pressure. The calculations have been made both with the norm-conserving method and with the projector augmented wave method with semicore electrons, giving identical results. Besides, the calculated volumes are in good agreement with those calculated by Yu *et al.* [13]. The GGA-PBE functional used has been shown to generally overestimate the volume of metals [43] and thermal contraction from 300 down to 0 K cannot account for such a large volume mismatch between experiments and calculations.

### B. Volume expansion per hydrogen atoms

In CrH, neutron-diffraction studies have shown that the hydrogen atoms occupy the octahedral sites of the *hcp* lattice [25,33]. The volume expansion accompanying the transition from  $\alpha$ -Cr to  $\epsilon$ -CrH as a function of pressure is given by the subtraction of the equation of state (EOS) fitted for pure chromium from the volume data of CrH. The result can be seen in Fig. 4. As already pointed out by Fukai [8], one needs to take into account the volume difference already induced by the *bcc* to *hcp* reorganization of the metallic framework to correctly estimate the value of the volume expansion caused by the insertion of a hydrogen atom inside an octahedral site of the *hcp* structure. According to DFT calculations, the volume of a hypothetical *hcp* Cr is higher by  $0.36 \text{ \AA}^3$  than that of

TABLE I. Volume, bulk modulus, and its first pressure derivative at ambient conditions for the different chromium hydrides. \*indicates electrochemical synthesis.

Phase	Space group	$V_0$ ( $\text{\AA}^3$ )	$B_0$ (GPa)	$B'_0$	Reference
Cr	$Im-3m$	12.00(0.02)	200(2)	4.3	experimental
			245(7)	5.5	Tkacz [26]
		11.55	258(0.5)	4.30(0.01)	DFT
$\epsilon$ -CrH	$P6_3/mmc$	14.23(0.02)	177(7)	4.7	experimental
			240(7)		Tkacz [26]
		13.43	249(0.5)	4.37(0.01)	DFT
		13.42			DFT [13]
		14.20*			[20]
		14.14*			$\text{CrH}_{0.961-0.996}$ [22]
		14.12*			$\text{CrH}_1$ [41]
		14.14*			$\text{CrH}_{0.97}$ [42]
		14.18			$\text{CrH}_{-1}$ [28]
14.19*			$\text{CrH}_{0.98}$ [25]		
$\text{Cr}_2\text{H}_3$	$C2/m$	14.78	218(0.5)	4.46	DFT
$\text{CrH}_2$	$Pnma$	17.4(0.5)	130(30)	5.2	experimental
		16.24	193(0.5)	4.49(0.01)	DFT

*bcc* Cr at 0 GPa. The hydrogen-induced volume expansion at ambient pressure would then be  $\sim 1.8 \text{ \AA}^3$ , which is in fairly good agreement with what is commonly found for *d*-band metals:  $2.2 \pm 0.4 \text{ \AA}^3$  for *O*-site occupancy and  $2.9 \pm 0.3 \text{ \AA}^3$  for *T*-site occupancy (cf. [8], Table 4.2). However, this volume expansion significantly decreases under pressure.

The volume expansion due to the dissolution of hydrogen inside CrH to form  $\text{Cr}_2\text{H}_3$  and  $\text{CrH}_2$  is estimated by subtracting the Vinet fit of the CrH EOS from the EOS data points of the corresponding hydride. As seen in Fig. 4, this operation

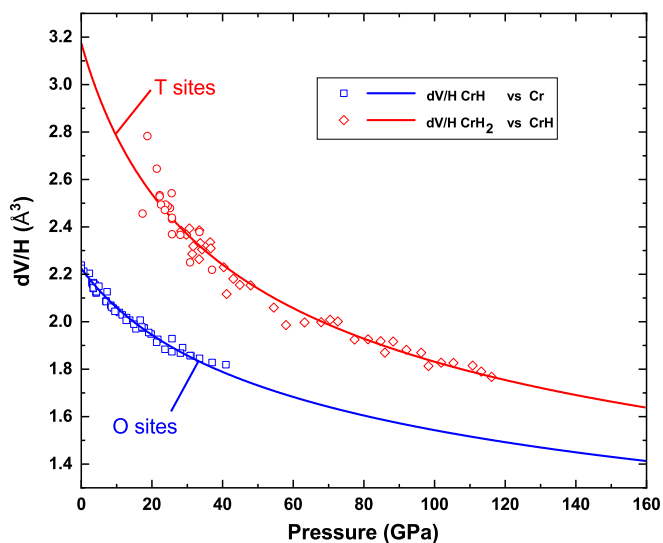


FIG. 4. Volume expansion per hydrogen atom for CrH,  $\text{Cr}_2\text{H}_3$ , and  $\text{CrH}_2$  as a function of pressure. Points are obtained through a subtraction of the fitted EOS of Cr from experimental data points of CrH and of the fitted EOS of CrH from experimental data points of  $\text{Cr}_2\text{H}_3$  and  $\text{CrH}_2$ . Lines are obtained through a subtraction between fitted EOS (not available for  $\text{Cr}_2\text{H}_3$ ).

results in data points for  $\text{Cr}_2\text{H}_3$  and  $\text{CrH}_2$  falling on a common curve, which is clearly different from the one corresponding to a hydrogen atom occupying an octahedral site. Indeed, following the structural prediction of Yu *et al.* [13],  $\text{Cr}_2\text{H}_3$  and  $\text{CrH}_2$  are formed by the hydrogen filling of the tetrahedral site of  $\epsilon$ -CrH hydride. This process is associated to a small monoclinic and orthorhombic distortion of the chromium *hcp* lattice for respectively  $\text{Cr}_2\text{H}_3$  and  $\text{CrH}_2$ . Due to the lack of data points at low pressure, the volume expansion of the metal lattice associated to a hydrogen atom occupying a tetrahedral site at ambient pressure was estimated thanks to the  $V_0$  of  $\text{CrH}_2$  which was set to the value minimizing the error but remaining within the commonly accepted values for *T*-site occupancy. Again, this volume expansion is a decreasing function of pressure. We believe that these two hydrogen volume expansion curves for octahedral and tetrahedral sites reflect a general behavior and could be useful to determine the hydrogen stoichiometry and hydrogen atoms positions in future experimental data on high-pressure hydrides.

### C. No $\text{CrH}_3$ observed

One must distinguish between two different mechanisms that occur under pressure to increase the hydrogen stoichiometry of a metal, and therefore two categories of hydrides can form. The “interstitial hydrides” which are the hydrides formed by dissolving hydrogen inside the interstitial sites of a structure (of the pure metal or of one of its hydrides) and the “reorganized hydrides” which are the hydrides that are stabilized thanks to a complete reconstructive transition of the metallic lattice. The case of chromium is very interesting, as the numerical study by Yu *et al.* [13] has predicted that *bcc* chromium under an excess of hydrogen should form both interstitial hydrides and reorganized hydrides, as the pressure increases. The relative stability range of each predicted chromium hydride is shown in Fig. 5. Upon pressure increase, interstitial hydrides were predicted to form by populating the tetrahedral sites of the

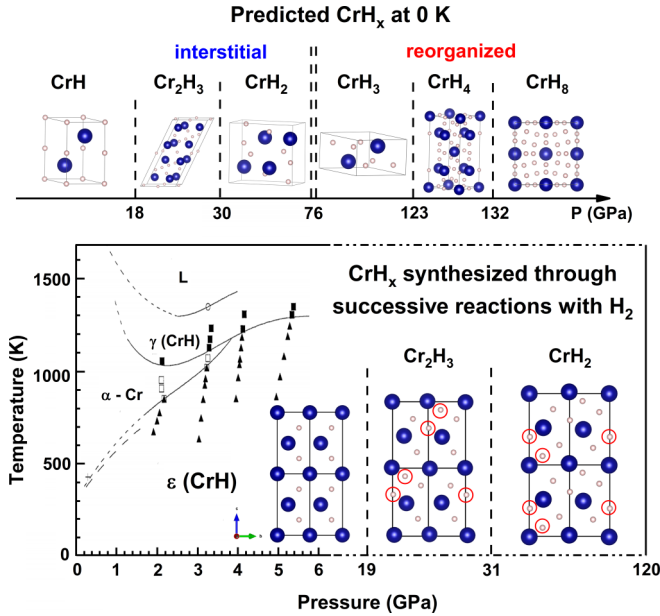


FIG. 5. Predicted chromium hydrides and their relative stability pressure ranges, as proposed in [13], compared to experimentally found chromium hydrides up to 120 GPa. The experimentally found  $\text{Cr}_2\text{H}_3$  and  $\text{CrH}_2$  chromium hydrides are identical to the predicted ones. Their structures are represented with the nearly ideal *hcp* cell formed by chromium atoms (not the real cell of the structure) and red circles indicate the positions of the inserted hydrogen atoms inside the cell. The latest published experimental low-pressure pressure-temperature data on the two allotropes of  $\text{CrH}$  are from Ref. [30]. Those data are nevertheless in contradiction with several studies regarding thermodynamics [31] and the volume of  $\gamma$ - $\text{CrH}$  [24,25], which calls for a new low-pressure high-temperature fine experimental study on the Cr-H system, as already done for the Mo-H system [32].

$\epsilon$ -*hcp*  $\text{CrH}$  phase. The  $\text{CrH}_2$  stoichiometry was predicted to be stable above 30 GPa, preceded by the formation of the intermediate compound  $\text{Cr}_2\text{H}_3$  at 18 GPa. As discussed above, these two hydrides have been observed. By further increasing pressure, reorganized hydrides were predicted to be stable. In particular,  $\text{CrH}_3$  should have formed above 76 GPa in our experiments but it was not observed when  $\text{CrH}_2$  was compressed in excess hydrogen up to 120 GPa and laser heating it at 100 GPa. This is all the more surprising as the predictions for interstitial hydrides have been verified with experimental and predicted transition pressures in relatively good agreement. Similarly, for the other group-VI transition metal, tungsten, *ab initio* calculations had predicted the stability of a rich variety of polyhydrides,  $\text{WH}_2$ ,  $\text{WH}_4$ , and  $\text{WH}_6$ , but none was observed over the pressure range of their calculated stability, even after laser heating the sample to overcome kinetic barriers [12]. Only *hcp*  $\text{WH}$  (in fact up to  $\text{WH}_{1.33}$  [11]) was found to be experimentally stable under pressure. The explanation provided by Zaleski-Ejgierd *et al.* is that the stability of the numerically found hydrides is based only on 0 K enthalpy difference considerations. At 300 K, one has to take into account the Gibbs energy with the corresponding entropy changes.

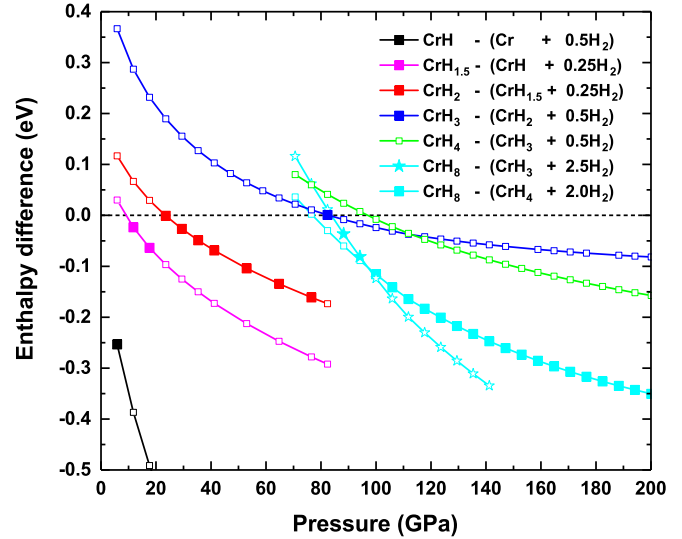


FIG. 6. Ground-state enthalpies of formation of the  $\text{CrH}_x$  structures with respect to the previous most stable chromium hydride and pure hydrogen (without zero-point energy). Filled symbols represent the stability domain of each new stoichiometry. Enthalpies are given per chromium atom.

In Fig. 6, we report the enthalpy difference calculated for the various consecutive chromium hydride formation reactions after structural optimization at several pressure points. The enthalpy difference accounting for the stability of  $\text{CrH}_3$  and  $\text{CrH}_4$  has a small pressure slope and does not exceed 100 meV until above 140 GPa. Hence, the amount of  $T\Delta S$  could be sufficient enough to disfavor  $\text{CrH}_3$  with respect to  $\text{CrH}_2 + 0.5\text{H}_2$ , especially if laser heating is applied to the sample to overcome large energy or kinetic barriers. The same problem could also occur for  $\text{CrH}_4$ . It is beyond the scope of this paper to quantitatively estimate this entropy effect. We could only venture to say that the predicted stability of  $\text{CrH}_8$  would probably be less affected. Indeed, its corresponding enthalpy difference with pressure has a steeper slope and largely exceeds 100 meV above 120 GPa. However, as shown by Yu *et al.* [13], zero-point energy should highly destabilize  $\text{CrH}_8$  and pressure in excess of 160 GPa should be necessary to observe it.

## V. CONCLUSION

The synthesis of two chromium hydrides is reported:  $\text{Cr}_2\text{H}_3$  is observed at 19 GPa and  $\text{CrH}_2$  above 31 GPa.  $\text{CrH}_2$  is the first dihydride for group-VI transition metal while  $\text{WH}_2$  and  $\text{MoH}_2$  were not observed in previous high-pressure studies. By measuring the EOS of Cr,  $\text{CrH}$ ,  $\text{Cr}_2\text{H}_3$ , and  $\text{CrH}_2$ , the pressure evolution of the volume expansions per hydrogen atom occupying octahedral and tetrahedral sites has been found. Finally, although nonstoichiometric  $\text{CrH}_{0.97}$  was not found to be superconductive [42], stoichiometric  $\text{CrH}$  was predicted to be superconductive at 10 K at ambient pressure [13]. Preliminary measurements have been carried out on  $\text{CrH}$  using the miniature DAC especially designed for superconductivity detection in a MPMS 3 superconducting quantum

interference device magnetometer and described in Ref. [44]. No superconductivity was observed down to 4 K in CrH. The magnetic measurements of the superconductive properties of Cr<sub>2</sub>H<sub>3</sub> and CrH<sub>2</sub> are under progress and will be the subject of a future publication.

## ACKNOWLEDGMENTS

The authors acknowledge the European Synchrotron Radiation Facility for provision of synchrotron radiation facilities. More particularly, we would like to thank M. Mezouar and V. Svitlyk for their precious assistance in using beamline ID27.

- 
- [1] D. Duan, Y. Liu, Y. Ma, Z. Shao, B. Liu, and T. Cui, *Natl. Sci. Rev.* **4**, 121 (2016).
- [2] A. Shamp and E. Zurek, *Novel Supercond. Mater.* **3**, 14 (2017).
- [3] F. Peng, Y. Sun, C. J. Pickard, R. J. Needs, Q. Wu, and Y. Ma, *Phys. Rev. Lett.* **119**, 107001 (2017).
- [4] H. Liu, I. I. Naumov, R. Hoffmann, N. W. Ashcroft, and R. J. Hemley, *Proc. Natl. Acad. Sci. USA* **114**, 6990 (2017).
- [5] A. P. Drozdov, M. I. Eremets, I. A. Troyan, V. Ksenofontov, and S. I. Shylin, *Nature (London)* **525**, 73 (2015).
- [6] C. M. Pépin, G. Geneste, A. Dewaele, M. Mezouar, and P. Loubeyre, *Science* **357**, 382 (2017).
- [7] C. M. Pépin, A. Dewaele, G. Geneste, P. Loubeyre, and M. Mezouar, *Phys. Rev. Lett.* **113**, 265504 (2014).
- [8] Y. Fukai, *The Metal-Hydrogen System*, Springer Series in Materials Science Vol. 21 (Springer-Verlag, Berlin, 2005).
- [9] M. Kuzovnikov and M. Tkacz, *Int. J. Hydrogen Energy* **42**, 340 (2017).
- [10] B. Li, Y. Ding, D. Y. Kim, R. Ahuja, G. Zou, and H.-K. Mao, *Proc. Natl. Acad. Sci. USA* **108**, 18618 (2011).
- [11] T. Scheler, F. Peng, C. L. Guillaume, R. T. Howie, Y. Ma, and E. Gregoryanz, *Phys. Rev. B* **87**, 184117 (2013).
- [12] P. Zaleski-Ejgierd, V. Labet, T. A. Strobel, R. Hoffmann, and N. W. Ashcroft, *J. Phys.: Condens. Matter* **24**, 155701 (2012).
- [13] S. Yu, X. Jia, G. Frapper, D. Li, A. R. Oganov, Q. Zeng, and L. Zhang, *Sci. Rep.* **5**, 17764 (2015).
- [14] X. Feng, J. Zhang, H. Liu, T. Iitaka, K. Yin, and H. Wang, *Solid State Commun.* **239**, 14 (2016).
- [15] M. Kuzovnikov, H. Meng, and M. Tkacz, *J. Alloys Compd.* **694**, 51 (2017).
- [16] R. J. Van Zee, T. C. DeVore, and W. Weltner, Jr., *J. Chem. Phys.* **71**, 2051 (1979).
- [17] X. Wang and L. Andrews, *J. Phys. Chem. A* **107**, 570 (2003).
- [18] L. Gagliardi and P. Pyykkö, *J. Am. Chem. Soc.* **126**, 15014 (2004).
- [19] T. Weichselfelder, *Justus Liebigs Ann. Chem.* **447**, 64 (1926).
- [20] C. A. Snavely, *Trans. Electrochem. Soc.* **92**, 537 (1947).
- [21] C. A. Snavely and D. A. Vaughan, *J. Am. Chem. Soc.* **71**, 313 (1949).
- [22] A. Knödler, *Metalloberfläche* **17**, 161 (1963).
- [23] M. Venkatraman and J. Neumann, *J. Phase Equilib.* **12**, 672 (1991).
- [24] A. D. Stock and K. I. Hardcastle, *J. Inorg. Nucl. Chem.* **32**, 1183 (1970).
- [25] V. Antonov, A. Beskrovnyy, V. Fedotov, A. Ivanov, S. Khasanov, A. Kolesnikov, M. Sakharov, I. Sashin, and M. Tkacz, *J. Alloys Compd.* **430**, 22 (2007).
- [26] M. Tkacz, *Rev. High Pressure Sci. Technol.* **7**, 263 (1998).
- [27] B. Baranowski and K. Bojarski, *Rocz. Chem.* **46**, 525 (1972).
- [28] B. Baranowski, K. Bojarski, and M. Tkacz, in *Proceedings of the Fourth International Conference on High Pressure, Kyoto, 1974* (Physico-Chemical Society of Japan, Kyoto, 1975), pp. 577–579.
- [29] E. Ponyatovsky and I. Belash, *Dokl. Akad. Nauk SSSR* **229**, 1171 (1976).
- [30] Y. Fukai and M. Mizutani, *Mater. Trans.* **43**, 1079 (2002).
- [31] V. Antonov and I. Sholin, *J. Alloys Compd.* **645**, S160 (2015).
- [32] S. Abramov, V. Antonov, B. Bulychiev, V. Fedotov, V. Kulakov, D. Matveev, I. Sholin, and M. Tkacz, *J. Alloys Compd.* **672**, 623 (2016).
- [33] G. Albrecht, F.-D. Doenitz, K. Klainstueck, and M. Betzl, *Phys. Status Solidi B* **3**, K249 (1963).
- [34] K. Takemura and A. Dewaele, *Phys. Rev. B* **78**, 104119 (2008).
- [35] C. Prescher and V. B. Prakapenka, *High Pressure Res.* **35**, 223 (2015).
- [36] J. Rodríguez-Carvajal, *Physica B: Condens. Matter* **192**, 55 (1993).
- [37] X. Gonze, G.-M. Rignanese, M. Verstraete, J.-M. Beuken, Y. Pouillon, R. Caracas, F. Jollet, M. Torrent, G. Zerah, M. Mikami, P. Ghosez, M. Veithen, J.-Y. Raty, V. Olevano, F. Bruneval, L. Reining, R. Godby, G. Onida, D. R. Hamann, and D. C. Allan, *Z. Kristallogr. - Cryst. Mater.* **220**, 558 (2005).
- [38] D. R. Hamann, *Phys. Rev. B* **88**, 085117 (2013).
- [39] J. P. Perdew, K. Burke, and M. Ernzerhof, *Phys. Rev. Lett.* **77**, 3865 (1996).
- [40] H. Sugimoto and Y. Fukai, *Acta Metall. Mater.* **40**, 2327 (1992).
- [41] R. J. Roy and T. R. Gibb, *J. Inorg. Nucl. Chem.* **29**, 341 (1967).
- [42] H. Khan and C. Raub, *J. Less-Common Met.* **49**, 399 (1976).
- [43] A. Dewaele, M. Torrent, P. Loubeyre, and M. Mezouar, *Phys. Rev. B* **78**, 104102 (2008).
- [44] A. Marizy, B. Guigue, F. Occelli, B. Leridon, and P. Loubeyre, *High Pressure Res.* **37**, 465 (2017).